JOURNAL OF COMPUTATIONAL PHYSICS 100, 270–283 (1992)

Interactions of an Elastic Solid with a Viscous Fluid: Eigenmode Analysis

R. M. S. M. SCHULKES*

Department of Mathematics, Delft University of Technology, P.O. Box 356, 2600 AJ Delft, The Netherlands

Received June 1, 1990; revised March 28, 1991

In this paper we study the interaction of a viscous fluid with an elastic solid. Of particular interest are the eigenmodes of the coupled system. Starting from the Navier–Stokes equations for the fluid and the linear elasticity equations for the solid, we derive the linear equations governing the motion of the system. It is shown how a variational formulation of the problem may be obtained by re-scaling the displacement unknowns. The finite-element technique is then used to discretize the equations. The resulting quadratic eigenvalue problem is solved by means of an inverse iteration procedure.

1. INTRODUCTION

The coupled motion of a fluid and a flexible structure is an important problem which occurs in various engineering applications. This is exemplified by the vast amount of literature which exists dealing with various types of fluid–structure interaction problems. The literature can be divided into two main areas, namely, papers dealing with non-linear fluid–structure interaction problems and papers dealing with the linearized problem. We will not be concerned with non-linear interaction problems; for work in this area the reader is referred to Liu and Chang [1] among many others.

Regarding literature dealing with linear fluid–structure interaction problems a further subdivision is possible. We identify the class of papers in which the governing equations are solved using numerical integration techniques to evaluate the time-dependent motion of the fluid and the solid and, on the other hand, there are papers in which the time-dependent problem is transformed to a problem in a frequency domain. In this paper we will restrict ourselves to the latter class of problems; for an overview of the former the reader is referred to Belytschko [2].

When dealing with the linear fluid–structure interaction problem in a frequency domain one is interested in the influence of the fluid on the eigenmodes of the structure and vice versa. Also of interest is how the structure is deflected when the fluid oscillates in one of its eigenmodes and what happens when one of the principal eigenmodes of the fluid is near a principal mode of the structure. In Table I an overview is given of some fluid–structure interaction papers in which eigenmodes of the coupled system are considered. In the papers the general emphasis is on calculating modal deflections and eigenfrequencies of the structure. The fluid motion resulting from modal vibrations of the structure has been investigated by Hamdi *et al.* [7] and Schulkes [12]. We note that a variety of models for the structure-part of the problem have been used. On the other hand, the fluid-part of the problem has been dealt with mainly by neglecting viscous effects. When damping characteristics of the fluid–structure system are to be investigated, viscosity is, however, important. Su [9] argues, in addition, that the hydrodynamic forces on the structure due to the boundary layer which forms in the vicinity of the structure, may also affect vibration characteristics of the system. For a fundamental mathematical treatment of vibrations of coupled systems including viscous effects, the reader is referred to Sanchez Hubert and Sanchez Palencia [13].

In this paper we will consider the motion of an incompressible, viscous fluid in an open flexible container. The container wall is modelled by an elastic solid. In Section 2 the problem to be considered is introduced and the governing equations are presented. In Section 3 a number of qualitative properties of the spectral problem, which results from the linearized Navier–Stokes equations coupled with the elasticity equations, are derived. We find that three types of normal modes exist, namely modes related to free surface oscillations, modes related to solid vibrations, and coupled fluid–solid modes. The three types of modes have different damping characteristics and depend differently on the parameters. Section 4 deals with the discrete eigenvalue problem obtained after a finite element discretization has been applied. The eigenvalue problem is solved using an inverse iteration procedure. In Section 5 numerical results

* Present address: D.A.M.T.P., Silver Street, CB3 9EW Cambridge, England.

0021-9991/92 $5.00

TABLE I

Author	Fluid model	Structure model
Miles [3]	Inviscid, incompressible	Simple beam
Coale [4]	Inviscid, incompressible	Shell
Boujot [5]	Inviscid, incompressible	Elastic solid
Berger *et al.* [6]	Inviscid, incompressible	Elastic solid
Hamdi *et al.* [7]	Inviscid, compressible	Elastic solid
Morand & Ohayon [8]	Inviscid, compressible	Elastic solid
Su [9]	Viscous, compressible	Shell
Deneuvy [10]	Inviscid, compressible	Thick plate
Capodanno [11]	Inviscid, incompressible	Membrane
Schulkes [12]	Viscous, incompressible	Membrane

are presented. The validity of an approximate expression due to Tong [14] to obtain symmetric matrices is investigated numerically, and phenomena related to the viscosity of the fluid are studied.

2. PROBLEM FORMULATION

Consider a region Ω which is divided into two regions Ω_1 and Ω_2 such that $\Omega = \Omega_1 \cup \Omega_2$ and $\Omega_1 \cap \Omega_2 = G$, as shown in Fig. 2.1. Let the region Ω_1 be occupied by a viscous fluid and assume that Ω_2 is occupied by an elastic solid. The boundary of Ω_1, denoted by $\partial\Omega_1$, consists of a free surface S, a rigid boundary W_f and the interfacial boundary G, i.e., $\partial\Omega_1 = S \cup W_f \cup G$. Likewise, the boundary of Ω_2, $\partial\Omega_2$, consists of a rigid part W_s, an unconstrained surface F, and the interfacial boundary G, i.e., $\partial\Omega_2 = G \cup W_s \cup F$. Furthermore, let $\mathbf{n}$ denote the outward unit normal to Ω and let τ be the unit tangent to $\partial\Omega$ directed counterclockwise from $\mathbf{n}$.

The equations describing the fluid motion in Ω_1 are the Navier–Stokes equations

$$\frac{\partial \mathbf{u}}{\partial t} + (\mathbf{u}\cdot\nabla)\mathbf{u} + \frac{1}{\rho_f}\nabla p = \nu\nabla^2\mathbf{u} + \mathbf{f}, \tag{2.1}$$

and the incompressibility condition

$$\nabla\cdot\mathbf{u} = 0. \tag{2.2}$$

In the above equations $\mathbf{u}$ denotes the fluid velocity, p the pressure, $\mathbf{f}$ the external body force, ρ_f the density, and

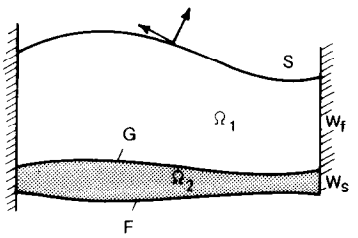

FIG. 2.1. Schematic diagram.

$\nu = \mu/\rho_f$ the kinematic viscosity of the fluid. On the free surface S we have the conditions that the normal stress in the fluid is equal to the outside gas pressure and the gas is not able to resist tangential stresses, thus

$$\sigma_n = -p_g, \qquad \sigma_\tau = 0. \tag{2.3}$$

Here p_g denotes the outside gas pressure and σ_n, σ_τ denote the normal and tangential stresses, respectively. We have used the notation

$$\sigma_n = \sum_{i,j=1}^{2} \sigma_{ij} n_i n_j, \qquad \sigma_\tau = \sum_{i,j=1}^{2} \sigma_{ij} n_i \tau_j,$$

in which n_i, τ_i, $i = 1, 2$, are the components of the outward unit normal and unit tangent, respectively, and

$$\sigma_{ij} = -p\delta_{ij} + \mu\left(\frac{\partial u_i}{\partial x_j} + \frac{\partial u_j}{\partial x_i}\right),$$

denotes the Cauchy stress tensor. On the free surface we also have the kinematic condition

$$\frac{D}{Dt}\alpha(\mathbf{x}, t) = 0, \tag{2.4}$$

in which $\alpha(\mathbf{x}, t) = \mathbf{n}\cdot(\mathbf{x}_S - \mathbf{x}) = 0$ is the equation of the free surface S ($\mathbf{x}_S$ is the position vector of S) and D/Dt denotes the Lagrangian derivative. On the rigid boundary W_f the no-slip condition characteristic of viscous flows is prescribed, viz.,

$$\mathbf{u} = 0. \tag{2.5}$$

The fluid is assumed to be incompressible so that the total quantity of liquid, V_f, remains constant, hence

$$\int_{\Omega_1} dx = V_f. \tag{2.6}$$

Next consider the equations governing the motion of the elastic solid in Ω_2. Assuming linear elasticity relations we find, cf. Landau and Lifshitz [15],

$$\rho_s \frac{\partial^2 \mathbf{d}}{\partial t^2} - \nabla\cdot\mathbf{T} = \mathbf{f}, \tag{2.7}$$

where $\mathbf{d}$ is the displacement vector of a particle in Ω_2, ρ_s is the density of the solid, and

$$T_{ij} = \frac{E}{1+\sigma}e_{ij} + \frac{E\sigma}{(1+\sigma)(1-2\sigma)}e_{kk}\delta_{ij},$$

$$e_{ij} = \frac{1}{2}\left(\frac{\partial d_i}{\partial x_j} + \frac{\partial d_j}{\partial x_i}\right)$$

denotes the stress tensor of the solid. E is Young's modulus and σ denotes Poisson's ratio. On the fixed boundary W_s the elastic solid is not displaced so that

$$\mathbf{d} = 0, \tag{2.8}$$

while on the unconstrained surface F the following conditions are given:

$$T_n = -p_g, \qquad T_\tau = 0. \tag{2.9}$$

The same notation as for the stress tensor of the fluid is used.

Finally consider the conditions on the interfacial boundary G. Let $\mathbf{n}_1$ denote a unit normal to G directed outward from Ω_1 and let $\boldsymbol{\tau}_1$ denote a unit tangent to G directed counterclockwise from $\mathbf{n}_1$. Likewise, $\mathbf{n}_2$ is a unit normal to G directed outward from Ω_2 and $\boldsymbol{\tau}_2$ is a unit tangent to G in the counterclockwise direction form $\mathbf{n}_2$. Demanding continuity of stresses across the interfacial boundary G we obtain

$$\sigma_{n_1} = T_{n_1}, \qquad \sigma_{\tau_1} = T_{\tau_1}. \tag{2.10}$$

Note that we have used $\mathbf{n}_1$, $\boldsymbol{\tau}_1$ to define the normal and tangential stresses on G. However, since $\mathbf{n}_1 = -\mathbf{n}_2$ and $\boldsymbol{\tau}_1 = -\boldsymbol{\tau}_2$, it follows that the subscripts n_1, τ_1 in (2.10) may be replaced by n_2 and τ_2. In addition to the continuity of stresses we have the no-cavitation condition; i.e., the fluid remains in contact with the solid at all times, hence

$$\frac{D}{Dt}(\mathbf{x}_G - \mathbf{x}) = 0, \tag{2.11}$$

where $\mathbf{x}_G$ denotes the position vector of G.

Solving the non-linear set of Eq. (2.1)–(2.11) is beyond the scope of this paper. Let us therefore first consider the equations of the static problem after which small perturbations with respect to this static configuration are investigated. Putting $\mathbf{u} \equiv 0$ we obtain from (2.1)

$$\frac{1}{\rho_f}\nabla p^0 = \mathbf{f}, \tag{2.12}$$

the conditions on S^0 reduce to

$$p^0 = p_g, \tag{2.13}$$

and the conditions on the static interface G^0 read

$$T^0_{n_1} = -p^0, \qquad T^0_{\tau_1} = 0. \tag{2.14}$$

The elasticity equation becomes

$$-\nabla \cdot \mathbf{T}^0 = \mathbf{f}, \tag{2.15}$$

with the condition on F^0

$$T^0_n = -p_g. \tag{2.16}$$

In the above and subsequent equations the superscript 0 refers to static parameters. Equations (2.12)–(2.16), together with the volume constraint (2.6), completely define the pressure at any point in the fluid, the stresses in the solid, and the static configuration of the boundaries F^0, G^0, and S^0. It will be evident that solving (2.12)–(2.16) is a non-trivial problem even for simple configurations. We will not attempt to solve this problem but assume, instead, that a static configuration is given.

We take $\mathbf{f} = -g\hat{\mathbf{k}}$, where $\hat{\mathbf{k}}$ is the unit vector pointing along the positive y-axis and g the gravitational acceleration. Surface tension effects on S^0 are neglected so that the free surface is flat and perpendicular to the y-axis. Let us now perturb the static configuration such that the position vectors of S and F are given by

$$\mathbf{x}_S = \mathbf{x}_{S^0} + \eta \mathbf{n}_S,$$

and

$$\mathbf{x}_G = \mathbf{x}_{G^0} + \mathbf{d}_G.$$

Here η is the small normal displacement from S^0, $\mathbf{n}_S$ is a unit normal to S^0, and $\mathbf{d}_G$ is a small displacement from the static interface. Substituting the above expressions for $\mathbf{x}_S$ and $\mathbf{x}_G$ into (2.4) and (2.11), using the steady state relations (2.12)–(2.16), and neglecting quantities which are of second-order smallness, we obtain the linearized equations governing the motion of the fluid and the elastic solid. In dimensionless form we have for the fluid

$$\left.\begin{aligned} \frac{\partial \mathbf{u}}{\partial t} + \nabla p &= \frac{1}{Re}\nabla^2 \mathbf{u} \\ \nabla \cdot \mathbf{u} &= 0 \end{aligned}\right\} \quad \text{in} \quad \Omega_1^0, \tag{2.17}$$

$$\left.\begin{aligned} \sigma_n &= -\eta \\ \sigma_\tau &= 0 \\ \mathbf{u} \cdot \mathbf{n} &= \frac{\partial \eta}{\partial t} \end{aligned}\right\} \quad \text{on} \quad S^0, \tag{2.18}$$

$$\mathbf{u} = 0 \quad \text{on} \quad W_f, \tag{2.19}$$

for the solid

$$\frac{\partial^2 \mathbf{d}}{\partial t^2} = \tilde{E}\nabla \cdot \mathbf{T} \quad \text{in} \quad \Omega_2^0, \tag{2.20}$$

$$T_n = 0, \qquad T_\tau = 0 \quad \text{on} \quad F^0, \tag{2.21}$$

$$\mathbf{d} = 0 \quad \text{on} \quad W_s, \tag{2.22}$$

and for the interface

$$\left.\begin{aligned} \sigma_{n_1} &= \tilde{E} r_\rho T_{n_1} - \hat{\mathbf{k}} \cdot \mathbf{d}_G \\ \sigma_{\tau_1} &= \tilde{E} r_\rho T_{\tau_1} \\ \frac{\partial \mathbf{d}_G}{\partial t} &= \mathbf{u} \end{aligned}\right\} \quad \text{on} \quad G^0. \tag{2.23}$$

In the above equations, $Re = UL/\nu$ denotes the Reynolds number (L is a length scale and $U = \sqrt{gL}$ is a velocity scale), $r_\rho = \rho_s/\rho_f$ is the ratio of densities of the solid and the fluid, and $\tilde{E} = E/\rho_s gL$ is a measure of the ratio of elastic bending forces and gravitational forces.

3. VARIATIONAL FORMULATION AND THE SPECTRAL PROBLEM

Equations (2.17) and (2.20) subject to boundary conditions (2.18), (2.19), and (2.21)–(2.23) will be written in a variational formulation. To that end the following Green formulas are used: for the Stokes equations,

$$\begin{aligned} &\int_{\Omega_1^0} \left(\frac{\partial \mathbf{u}}{\partial t} + \nabla p - \frac{1}{Re} \nabla^2 \mathbf{u} \right) \cdot \mathbf{v} \, dx \\ &\quad = \int_{\Omega_1^0} \left(\frac{\partial \mathbf{u}}{\partial t} \cdot \mathbf{v} - p \nabla \cdot \mathbf{v} \right) dx + \frac{1}{Re} a(\mathbf{u}, \mathbf{v}) \\ &\quad - \int_{\partial \Omega_1^0} (\sigma_{n_1} v_{n_1} + \sigma_{\tau_1} v_{\tau_1}) \, ds, \end{aligned} \tag{3.1}$$

in which

$$\begin{aligned} a(\mathbf{u}, \mathbf{v}) = \frac{1}{2} \sum_{i,j=1}^{2} \int_{\Omega_1^0} &\left(\frac{\partial u_i}{\partial x_j} + \frac{\partial u_j}{\partial x_i} \right) \\ &\times \left(\frac{\partial v_i}{\partial x_j} + \frac{\partial v_j}{\partial x_i} \right) dx, \qquad x_1 = x, \, x_2 = y, \end{aligned}$$

and, for the linear elasticity relations,

$$\begin{aligned} &\int_{\Omega_2^0} \left(\frac{\partial^2 \mathbf{d}}{\partial t^2} - \tilde{E} \nabla \cdot \mathbf{T} \right) \cdot \mathbf{e} \, dx \\ &\quad = \int_{\Omega_2^0} \frac{\partial^2 \mathbf{d}}{\partial t^2} \cdot \mathbf{e} \, dx + \tilde{E} b(\mathbf{d}, \mathbf{e}) \\ &\quad - \int_{\partial \Omega_2^0} (\tilde{E} T_{n_2} e_{n_2} + \tilde{E} T_{\tau_2} e_{\tau_2}) \, ds, \end{aligned} \tag{3.2}$$

in which

$$b(\mathbf{d}, \mathbf{e}) = \frac{1}{2} \sum_{i,j=1}^{2} \int_{\Omega_2^0} T_{ij} \left(\frac{\partial e_i}{\partial x_j} + \frac{\partial e_j}{\partial x_i} \right) dx.$$

Let us assume that the time-dependence of $\mathbf{u}$, p, η, and $\mathbf{d}$ is of the form $e^{\lambda t}$, where λ is in general some complex quantity. Employing the Green formulas (3.1) and (3.2) and substituting the boundary conditions on $\partial\Omega_1^0$ and $\partial\Omega_2^0$ we obtain the variational formulation of equations (2.17)–(2.23), namely:

find $\mathbf{u} \in V_1$, $p \in Q$, and $\mathbf{d} \in V_2$ such that for all $\mathbf{v} \in V_1$, $q \in Q$, and $\mathbf{e} \in V_2$ the following equations are satisfied:

$$\begin{aligned} &\int_{\Omega_1^0} (\lambda \mathbf{u} \cdot \mathbf{v} - p \nabla \cdot \mathbf{v}) \, dx + \frac{1}{Re} a(\mathbf{u}, \mathbf{v}) + \frac{1}{\lambda} \int_{S^0} u_n v_n \, ds \\ &\quad - \int_{G^0} [(\tilde{E} r_\rho T_{n_1} - \hat{\mathbf{k}} \cdot \mathbf{d}) v_{n_1} + \tilde{E} r_\rho T_{\tau_1} v_{\tau_1}] \, ds = 0, \end{aligned} \tag{3.3}$$

$$\int_{\Omega_1^0} q \nabla \cdot \mathbf{u} \, dx = 0, \tag{3.4}$$

$$\lambda \mathbf{d} = \mathbf{u} \qquad \text{on} \quad G^0, \tag{3.5}$$

$$\begin{aligned} &\int_{\Omega_2^0} \lambda^2 \mathbf{d} \cdot \mathbf{e} \, dx + \tilde{E} b(\mathbf{d}, \mathbf{e}) \\ &\quad - \int_{G^0} (\tilde{E} T_{n_2} e_{n_2} + \tilde{E} T_{\tau_2} e_{\tau_2}) \, ds = 0. \end{aligned} \tag{3.6}$$

We have introduced the spaces of vector functions $V_1 = \{\mathbf{u} \in \Omega_1^0 : \mathbf{u} = 0 \text{ on } W_f\}$, $V_2 = \{\mathbf{d} \in \Omega_2^0 : \mathbf{d} = 0 \text{ on } W_s\}$ and the space of scalar functions $Q = \{q \in \Omega_1^0\}$. The functions in V_1, V_2, and Q must be so smooth that the integrals (3.3)–(3.6) exist. Observe that Eq. (3.3) and (3.6) both contain integrals over the interfacial boundary G^0 in which normal and tangential stresses appear. The terms containing the stresses can be eliminated in the following way. Take Eq. (3.6), multiply it by the density ratio r_ρ, and add the result to (3.3), giving

$$\begin{aligned} &\int_{\Omega_1^0} (\lambda \mathbf{u} \cdot \mathbf{v} - p \nabla \cdot \mathbf{v}) \, dx + \frac{1}{Re} a(\mathbf{u}, \mathbf{v}) \\ &\quad + r_\rho \int_{\Omega_2^0} \lambda^2 \mathbf{d} \cdot \mathbf{e} \, dx + r_\rho \tilde{E} b(\mathbf{d}, \mathbf{e}) \\ &\quad + \frac{1}{\lambda} \int_{S^0} u_n v_n \, ds \\ &\quad - \int_{G^0} [\tilde{E} r_\rho (T_{n_1} v_{n_1} + T_{n_2} e_{n_2} + T_{\tau_1} v_{\tau_1} \\ &\quad + T_{\tau_2} e_{\tau_2}) - \hat{\mathbf{k}} \cdot \mathbf{d} v_{n_1}] \, ds = 0. \end{aligned}$$

By virtue of the fact that $\mathbf{n}_1 = -\mathbf{n}_2$ and $\tau_1 = -\tau_2$ on G^0, it follows that the terms containing normal and tangential stresses in the integral over G^0 cancel when we demand that the test functions are identical on G^0, i.e., $\mathbf{v}|_{G^0} = \mathbf{e}|_{G^0}$.

Let us introduce a new variable $\mathbf{w}$, where $\mathbf{w}$ is defined as follows: $\mathbf{w}=\mathbf{u}$ in Ω_1^0 and $\mathbf{w}=\lambda\mathbf{d}$ in Ω_2^0. On making the substitution for $\mathbf{w}$, it follows that the continuity condition (3.5) on the interface is satisfied automatically. Therefore, instead of having four unknowns on the interface G^0 (two components of the velocity and two components of the displacement), just the two components of $\mathbf{w}$ are unknown. The variational equations (3.3)–(3.6) can now be written like

find $\mathbf{w}\in V$ and $p\in Q$ such that for all functions $\hat{\mathbf{v}}\in\hat{V}$ and $q\in Q$ the following equations are satisfied:

$$\int_{\Omega_1^0}(\lambda\mathbf{w}\cdot\hat{\mathbf{v}}-p\nabla\cdot\hat{\mathbf{v}})\,dx+\frac{1}{Re}a(\mathbf{w},\hat{\mathbf{v}})+r_\rho\int_{\Omega_2^0}\lambda\mathbf{w}\cdot\hat{\mathbf{v}}\,dx+\frac{1}{\lambda}r_\rho\tilde{E}b(\mathbf{w},\hat{\mathbf{v}})+\frac{1}{\lambda}\int_{S^0}w_n\hat{v}_n\,ds+\frac{1}{\lambda}\int_{G^0}\hat{\mathbf{k}}\cdot\mathbf{w}\hat{v}_{n_1}\,ds=0, \tag{3.7}$$

$$\int_{\Omega_1^0}q\nabla\cdot\mathbf{w}\,dx=0, \tag{3.8}$$

where $V=\{\mathbf{w}\in V_1\cup V_2\}$ and $\hat{V}=\{\mathbf{v}\in V_1,\mathbf{e}\in V_2,\ \mathbf{v}|_{G^0}=\mathbf{e}|_{G^0}\}$. Note that the test functions $\hat{\mathbf{v}}$ are not necessarily of the same form in the two domains Ω_1^0 and Ω_2^0. All we demand is that the restriction to the interfacial boundary G^0 of the different test functions must be identical. Introducing the unknown $\mathbf{w}$ is, more or less, natural. Namely, had we not changed to dimensionless variables we would have found the dimension of $\mathbf{w}$ to be equal to *length* $(time)^{-1}$ in both Ω_1^0 and Ω_2^0. That is, in the whole of the domain we are dealing with velocity unknowns.

General properties of the spectrum can be derived if we are able to write (3.7), (3.8) in the form of a functional which has to be minimized. The term containing the integral over G^0 in (3.7) is, however, non-symmetric which means that Eq. (3.7), as it stands, can not be written as a minimization problem. To overcome this difficulty we apply the so-called Tong-hypothesis [14], i.e., we assume that $\hat{\mathbf{k}}\cdot\mathbf{w}$ may be replaced by $(\hat{\mathbf{k}}\cdot\mathbf{n}_1)(\mathbf{w}\cdot\mathbf{n}_1)$. Note that when the unit normal $\mathbf{n}_1$ is parallel to $\hat{\mathbf{k}}$ the Tong-hypothesis is satisfied identically; in all other cases it is an approximation of questionable validity. Assume for the moment that the Tong-hypothesis is a reasonable first-order approximation. Solving Eq. (3.8) and (3.7) is then equivalent to finding the pair $(\mathbf{w},\lambda)$ such that the functional

$$\Phi(\mathbf{w},\lambda)=\lambda^2((\mathbf{w},\mathbf{w})_{\Omega_1^0}+r_\rho(\mathbf{w},\mathbf{w})_{\Omega_2^0})+\lambda\frac{1}{Re}a(\mathbf{w},\mathbf{w})+r_\rho\tilde{E}b(\mathbf{w},\mathbf{w})+(w_n,w_n)_{S^0}+(w_n,w_n)_{G^0}$$

assumes a stationary value equal to zero. We have introduced the notation

$$(\mathbf{w},\mathbf{w})_{\Omega_1^0}=\int_{\Omega_1^0}|\mathbf{w}|^2\,dx,$$

$$(w_n,w_n)_{S^0}=\int_{S^0}|w_n|^2\,ds,$$

$$(w_n,w_n)_{G^0}=\int_{G^0}\hat{\mathbf{k}}\cdot\mathbf{n}_1\,|w_{n_1}|^2\,ds,\qquad\text{etc.}$$

Take $\Phi\equiv 0$ and treat the resulting equation as a quadratic function in λ. Solving for λ we can derive the following qualitative properties concerning the spectrum of the fluid–structure interaction problem:

(i) If

$$r_\rho\tilde{E}b(\mathbf{w},\mathbf{w})+(w_n,w_n)_{S^0}+(w_n,w_n)_{G^0}>0,$$

then problem (3.8), (3.7) is stable with respect to infinitesimal perturbations;

(ii) If

$$\frac{1}{Re^2}a(\mathbf{w},\mathbf{w})^2\geqslant 4[(\mathbf{w},\mathbf{w})_{\Omega_1^0}+r_\rho(\mathbf{w},\mathbf{w})_{\Omega_2^0}]\times[r_\rho\tilde{E}b(\mathbf{w},\mathbf{w})+(w_n,w_n)_{S^0}+(w_n,w_n)_{G^0}],$$

then the eigenvalues corresponding to the eigenfunctions $\mathbf{w}$ are real and negative, which corresponds to an aperiodic damping process;

(iii) If

$$\frac{1}{Re^2}a(\mathbf{w},\mathbf{w})^2<4[(\mathbf{w},\mathbf{w})_{\Omega_1^0}+r_\rho(\mathbf{w},\mathbf{w})_{\Omega_2^0}]\times[r_\rho\tilde{E}b(\mathbf{w},\mathbf{w})+(w_n,w_n)_{S^0}+(w_n,w_n)^{G^0}],$$

then the eigenvalues are complex, occurring in complex-conjugate pairs. The real part of the eigenvalues is negative so that the oscillations are damped.

The stability condition (i) hinges on the positiveness of the various terms. One can easily show that the bilinear form $b(\cdot,\cdot)$ is V-elliptic, i.e.,

$$b(\mathbf{w},\mathbf{w})\geqslant\alpha\,\|\mathbf{w}\|_{V_2}^2\qquad\text{for all}\quad\mathbf{w}\in V_2,\ \alpha\in\mathbb{R}^+,$$

when the Poisson ratio $\sigma<\frac{1}{2}$. Since $(w_n,w_n)_{G^0}\geqslant-\int_{G^0}|w_n|^2\,ds$ it follows that (i) will always be satisfied when

$$r_\rho\tilde{E}b(\mathbf{w},\mathbf{w})+(w_n,w_n)_{S^0}>\int_{G^0}|w_n|^2\,ds.$$

Hence, provided $b(\cdot,\cdot)$ is V-elliptic we find that stability is guaranteed if $\tilde{E}$ is sufficiently large, that is, if the solid is sufficiently rigid. We note that if the solid rests upon the liquid then $(w_n, w_n)_{G^0} \geq 0$ so that V-ellipticity of $b(\cdot,\cdot)$ is sufficient to guarantee stability. The damping of the normal modes is characterized by the term $(1/Re)\, a(\mathbf{w}, \mathbf{w})$ which is proportional to the energy dissipation due to viscous effects. This is the only source of damping, since we have not included damping effects in the structure in our model.

Schulkes [12] has shown that in the case where the structure is modelled by a membrane there exist two types of oscillation modes, namely free-surface modes and structural-vibration modes. The free-surface oscillation modes were characterized by a significant displacement of the free-surface while the membrane was deflected only slightly. Membrane-vibration modes, on the other hand, are characterized by a significant displacement of the membrane while the free-surface is not necessarily effected significantly by the membrane motion. In order to investigate the properties of the eigenmodes in this paper we assume that it is also possible here to make the distinction between free-surface and structural-vibration modes.

Let us, first assume that normal modes exist such that $\mathbf{w}$ in Ω_2^0 is small. Neglecting all terms which refer to quantities in Ω_2^0 we obtain

$$\lambda = \frac{\left(\begin{array}{l} -(1/Re)\, a(\mathbf{w}, \mathbf{w}) \\ \quad \pm \sqrt{(1/Re^2)\, a(\mathbf{w}, \mathbf{w})^2 - 4(\mathbf{w}, \mathbf{w})_{\Omega_1^0} (w_n, w_n)_{S^0}} \end{array}\right)}{2(\mathbf{w}, \mathbf{w})_{\Omega_1^0}}. \tag{3.9}$$

Equation (3.9) is the expression for the eigenfrequencies of a viscous fluid in a rigid container in terms of the corresponding eigenfunctions, cf. Kopachevskii and Myshkis [16].

Assume, alternatively, that eigenmodes exist with corresponding eigenfunctions such that $\mathbf{w}$ in Ω_1^0 is small. Neglecting terms in the discriminant which refer to quantities in Ω_1^0 we obtain

$$\lambda = -\frac{a(\mathbf{w}, \mathbf{w})}{2Re\, r_\rho (\mathbf{w}, \mathbf{w})_{\Omega_2^0}} \pm \mathrm{i} \sqrt{\tilde{E} b(\mathbf{w}, \mathbf{w})/(\mathbf{w}, \mathbf{w})_{\Omega_2^0}}. \tag{3.10}$$

$\mathrm{Im}(\lambda)$ in (3.10) can readily be shown to be equivalent to the Rayleigh quotient for the case of a solid which experiences unconstrained vibrations. The eigenvalues given by (3.10) correspond therefore to eigenfunctions which represent structural vibrations which effect the fluid only slightly. Since $\mathbf{w}$ is assumed small in Ω_1^0 it follows that $\mathrm{Re}(\lambda)$ is small and hence the corresponding modes are weakly damped.

Finally, consider the case in which Re is large so that only terms to first order in $1/Re$ need be retained. Assume that normal modes exist such that on the interface G^0 the fluid and structure are displaced significantly while the free surface remains relatively undisturbed; i.e., we can neglect $(w_n, w_n)_{S^0}$. Assume, in addition, that $r_\rho \tilde{E} b(\mathbf{w}, \mathbf{w}) \gg (w_n, w_n)_{G^0}$ which can be achieved by choosing $\tilde{E}$ sufficiently large. Under the above assumptions λ is approximated by

$$\lambda = \frac{-a(\mathbf{w}, \mathbf{w})}{2Re[(\mathbf{w}, \mathbf{w})_{\Omega_1^0} + r_\rho (\mathbf{w}, \mathbf{w})_{\Omega_2^0}]} \pm \mathrm{i} \sqrt{r_\rho \tilde{E} b(\mathbf{w}, \mathbf{w})/((\mathbf{w}, \mathbf{w})_{\Omega_1^0} + r_\rho (\mathbf{w}, \mathbf{w})_{\Omega_2^0})}. \tag{3.11}$$

Since $\mathrm{Im}(\lambda) \sim \sqrt{\tilde{E}}$ it follows that the eigenmodes in (3.11) are related to structural vibration modes. The fluid inertia term $(\mathbf{w}, \mathbf{w})_{\Omega_1^0}$ in the denominator of $\mathrm{Im}(\lambda)$ in (3.11) is of interest. Namely, taking into account the fluid motion leads to an extra term in the denominator of $\mathrm{Im}(\lambda)$ when comparing Eq. (3.10) and (3.11). It follows that the imaginary parts of normal modes of a freely-vibrating structure are larger than the corresponding modes of a structure in contact with a fluid due to the inertia of the fluid. This observation is related to the concept of added mass, which refers to the procedure (applicable only in the case of non-viscous fluids) of eliminating the fluid unknowns by adding an inertia matrix to the mass matrix of the solid. See, for example, Deruntz and Geers [17] and Müller [18].

4. NUMERICAL SOLUTION BY THE FINITE-ELEMENT METHOD

Equations (3.7), (3.8) are solved using the finite-element technique. The incompressibility constraint will be dealt with by using a penalty-function approach; i.e., the variational integral (3.8) is written like (cf. Cuvelier *et al.* [19])

$$\varepsilon_p \int_{\Omega_1^0} pq \, dx + \int_{\Omega_1^0} q \nabla \cdot \mathbf{w} \, dx = 0. \tag{4.1}$$

Here, ε_p is some small penalty parameter, typically $\varepsilon_p \sim 10^{-6}$. Let us write Eqs. (3.7) and (4.1) in the following abbreviated way:

$$F(w_i, \hat{v}_i) - P^i(p, \hat{v}_i) + E(w_i, \hat{v}_i) = 0, \qquad i = 1, 2 \tag{4.2}$$

$$\varepsilon D(p, q) + P^1(q, w_1) + P^2(q, w_2) = 0. \tag{4.3}$$

We have used the notation

$$F(w_i, \hat{v}_i) = \int_{\Omega_1^0} (\lambda w_i \hat{v}_i \, dx) - \frac{1}{Re} a(w_i, \hat{v}_i) + \frac{1}{\lambda} \int_{S^0} (w_i n_i)(\hat{v}_i n_i) \, ds,$$

$$E(w_i, \hat{v}_i) = r_\rho \lambda \int_{\Omega_2^0} w_i \hat{v}_i \, dx + \frac{1}{\lambda} r_\rho \tilde{E} b(w_i, \hat{v}_i)$$

$$+ \frac{1}{\lambda} \int_{G^0} (k_i w_i)(\hat{v}_i n_i) \, ds = 0,$$

$$P^j(p, \hat{v}_i) = \int_{\Omega_1^0} p \frac{\partial \hat{v}_i}{\partial x_j} \, dx, \qquad D(p, q) = \int_{\Omega_1^0} pq \, dx.$$

We note that the functionals $F(w_i, \hat{v}_i)$, $P^j(p, \hat{v}_i)$, and $D(p, q)$ are defined only on the domain occupied by the fluid, i.e., on Ω_1^0 including G^0. On the other hand, $E(w_i, \hat{v}_i)$ is a functional defined only on the domain occupied by the elastic solid, i.e., on Ω_2^0 including G^0. For the construction of the finite-element approximation of $\mathbf{w}$ and p, we write w_i $(i = 1, 2)$ and p as the sum of usual finite-element basis functions with small support. The basis functions for w_i, denoted by $\phi_k(\mathbf{x})$, are divided into three sets. Namely, those which are non-zero at nodal points in $\Omega_1^0 \backslash G^0$ (K_f in number) and zero at the remaining nodal point, those which are non-zero only at the nodal points on G^0 (K_g in number), and those which are non-zero at nodal points in $\Omega_2^0 \backslash G^0$ (K_e in number) and zero elsewhere. Hence

$$w_i = \sum_{k=1}^{K_f} \tilde{w}_{ik} \phi_k(\mathbf{x}) + \sum_{k=K_f+1}^{K_f+K_g} \tilde{w}_{ik} \phi_k(\mathbf{x}) + \sum_{k=K_f+K_g+1}^{K_f+K_g+K_e} \tilde{w}_{ik} \phi_k(\mathbf{x})$$

$$p = \sum_{m=1}^{M} \tilde{p}_m \chi_m(\mathbf{x}),$$

where the basis functions $\chi_m(\mathbf{x})$ are non-zero only at the nodal points in Ω_1^0 and on G^0 (since the pressure is defined only in the fluid domain). For the test functions $\hat{v}_i$ we take $\phi_n(\mathbf{x})$ and for q we take $\chi_n(\mathbf{x})$. The discrete equivalents of Eq. (4.2) and (4.3) become, on substituting for w_i and p,

$$\sum_{k=1}^{K_f+K_g} \tilde{w}_{ik} F(\phi_k, \phi_n) - \sum_{m=1}^{M} \tilde{p}_m P^i(\chi_m, \phi_n) + \sum_{k=K_f+1}^{K_f+K_g+K_e} \tilde{w}_{ik} E(\phi_k, \phi_n) = 0,$$

$$i = 1, 2, \qquad n = 1, 2, \ldots, K_f + K_g + K_e, \tag{4.4}$$

$$\varepsilon \sum_{m=1}^{M} D(\chi_m, \chi_n) + \sum_{k=1}^{K_f+K_g} \tilde{w}_{1k} P^1(\chi_n, \phi_k) + \sum_{k=1}^{K_f+K_g} \tilde{w}_{2k} P^2(\chi_n, \phi_k) = 0, \qquad n = 1, 2, \ldots, M. \tag{4.5}$$

Let $\mathbf{w}_f^{(i)}$ $(i = 1, 2)$ denote the vectors containing the unknowns in the nodal points in $\Omega_1^0 \backslash G^0$. The vectors denoted by $\mathbf{w}_g^{(i)}$ $(i = 1, 2)$ contain unknowns in the nodal points on G^0 and $\mathbf{w}_e^{(i)}$ $(i = 1, 2)$ contain unknowns refering to nodal points in $\Omega_2^0 \backslash G^0$. Note $\mathbf{w}_f^{(i)}$, $\mathbf{w}_g^{(i)}$, and $\mathbf{w}_e^{(i)}$ are vectors of length K_f, K_g, and K_e, respectively. The explicit form of Eq. (4.4) is then given by

$$\begin{pmatrix} F_{ff} & 0 & F_{fg} & 0 & 0 & 0 \\ 0 & F_{ff} & 0 & F_{fg} & 0 & 0 \\ F_{gf} & 0 & F_{gg} & 0 & 0 & 0 \\ 0 & F_{gf} & 0 & F_{gg} & 0 & 0 \\ 0 & 0 & 0 & 0 & 0 & 0 \\ 0 & 0 & 0 & 0 & 0 & 0 \end{pmatrix} \begin{pmatrix} \mathbf{w}_f^{(1)} \\ \mathbf{w}_f^{(2)} \\ \mathbf{w}_g^{(1)} \\ \mathbf{w}_g^{(2)} \\ \mathbf{w}_e^{(1)} \\ \mathbf{w}_e^{(2)} \end{pmatrix} - \mathbf{P}^T \mathbf{p}$$

$$+ \begin{pmatrix} 0 & 0 & 0 & 0 & 0 & 0 \\ 0 & 0 & 0 & 0 & 0 & 0 \\ 0 & 0 & E_{gg} & 0 & E_{ge} & 0 \\ 0 & 0 & 0 & E_{gg} & 0 & E_{ge} \\ 0 & 0 & E_{eg} & 0 & E_{ee} & 0 \\ 0 & 0 & 0 & E_{eg} & 0 & E_{ee} \end{pmatrix} \begin{pmatrix} \mathbf{w}_f^{(1)} \\ \mathbf{w}_f^{(1)} \\ \mathbf{w}_g^{(2)} \\ \mathbf{w}_g^{(2)} \\ \mathbf{w}_e^{(1)} \\ \mathbf{w}_e^{(2)} \end{pmatrix} = 0 \tag{4.6}$$

and the penalized incompressibility constraint can be written as

$$\varepsilon \mathbf{D}\mathbf{p} + \mathbf{P} \begin{pmatrix} \mathbf{w}_f^{(1)} \\ \mathbf{w}_f^{(2)} \\ \mathbf{w}_g^{(1)} \\ \mathbf{w}_g^{(2)} \\ \mathbf{w}_e^{(1)} \\ \mathbf{w}_e^{(2)} \end{pmatrix} = 0. \tag{4.7}$$

The large matrices in Eq. (4.6) are square and of order $2(K_f + K_g + K_e)$, the components of the sub-matrices are given by

$$(F_{ff})_{ij} = F(\phi_i, \phi_j), \qquad 1 \leqslant i, j \leqslant K_f$$

$$(F_{gg})_{ij} = F(\phi_i, \phi_j), \qquad K_f + 1 \leqslant i, j \leqslant K_f + K_g$$

$$(E_{ee})_{ij} = E(\phi_i, \phi_j), \qquad K_f + K_g + 1 \leqslant i, j \leqslant K_f + K_g + K_e$$

$$\vdots$$

The matrix $\mathbf{P}$ in the momentum and the continuity equations is a non-square matrix of order $2(K_f + K_g + K_e) \times M$, with only the first $2(K_f + K_g)$-columns containing non-zero elements. Thus

$$\mathbf{P} = (\mathbf{P}^1, \mathbf{P}^2, 0),$$

where $\mathbf{P}^n$ $(n = 1, 2)$ are matrices of order $(K_f + K_g) \times M$ with components

$$(\mathbf{P}^n)_{ij} = P^n(\chi_i, \phi_j), \qquad 1 \leqslant i \leqslant M, \; 1 \leqslant j \leqslant K_f + K_g.$$

The matrix **D** is square and non-singular so that it may be inverted. Hence, the continuity equation (4.7) may be solved for the pressure in terms of the velocity unknowns so that the pressure unknowns can be eliminated entirely from the momentum equation (4.6).

Substituting the expressions for the functionals $F(w_i, \hat{v}_i)$ and $E(w_i, \hat{v}_i)$ into the momentum equations, we obtain a discrete eigenvalue problem of the form

$$(\lambda^2 \mathbf{A} + \lambda \mathbf{B} + \mathbf{C})\mathbf{x} = 0, \tag{4.8}$$

where

$$\mathbf{A} = \begin{pmatrix} M_{ff} & M_{fg} & 0 \\ M_{gf} & M_{gg} + M^*_{gg} & M^*_{ge} \\ 0 & M^*_{eg} & M^*_{ee} \end{pmatrix},$$

$$\mathbf{B} = \begin{pmatrix} A_{ff} & A_{fg} & 0 \\ A_{gf} & A_{gg} & 0 \\ 0 & 0 & 0 \end{pmatrix},$$

$$\mathbf{C} = \begin{pmatrix} S_{ff} & S_{fg} & 0 \\ S_{gf} & S_{gg} + G_{gg} + B_{gg} & B_{ge} \\ 0 & B_{eg} & B_{ee} \end{pmatrix}, \quad \mathbf{x} = \begin{pmatrix} \mathbf{w}_f \\ \mathbf{w}_g \\ \mathbf{w}_e \end{pmatrix}.$$

In the above equations the matrix M is the discrete equivalent of the fluid inertia term, the matrix A is that of the fluid stiffness term, including the penalty matrix $(1/\varepsilon_p)\,\mathbf{P}^T\mathbf{D}^{-1}\mathbf{P}$, and the matrix S refers to the integral over the free surface of the fluid. The matrix M^* refers to the solid inertia term, the matrix G to the integral over the interface, and the matrix B is the stiffness matrix of the solid. In the vector $\mathbf{x}$ the components of $\mathbf{w}_f$ refer to the fluid unknowns not including those on G^0, the components of $\mathbf{w}_g$ refer to the unknowns on G^0, and the components of $\mathbf{w}_e$ refer to the scaled unknowns in the elastic solid, again excluding those on G^0. The matrices **A**, **B**, and **C** are of order $2(K_f + K_g + K_e)$ with **A** symmetric and non-singular, **B** symmetric and singular with rank $2(K_f + K_g)$. The matrix **C** is, in general, non-symmetric (due to the anti-symmetry of G_{gg} if the Tong-hypothesis is not applied) and it is singular with rank equal to $2(K_g + K_e) + \text{rank}(S)$ ($\text{rank}(S) < 2K_f$, since only degrees of freedom on the free-surface S^0 give non-zero entries).

So far we have not discussed the types of elements used to discretize the regions Ω_1^0 and Ω_2^0 nor have we dealt with the particular forms of the basis functions. Regarding the element types we shall restrict ourselves to triangular elements in Ω_1^0 and Ω_2^0. For the particular form of the basis functions on the triangular elements, we first consider equations related to the fluid unknowns in Ω_1^0. In the variational formulation of the Stokes equations (3.1), only first-order partial derivatives occur, implying that linear basis functions for the approximation of w_i in Ω_1^0 are in principle sufficient

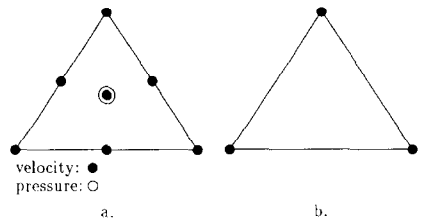

FIG. 4.1. Element for the fluid velocity and pressure (a) and for displacement unknowns (b).

(to ensure continuous differentiability element-wise and piece-wise continuity in Ω_1^0). However, the obvious demand that the velocity approximation be not completely described by the continuity equation forces higher order polynomials to be used for the basis functions for w_i in Ω_1^0 (cf. Cuvelier et al. [19]). Hence, for the finite-element approximation of the fluid velocity and the pressure, the so-called Crouzeix–Raviart element is used: the basis functions for the velocity are extended quadratic polynomials based on seven nodal points (one on each corner of the triangle, one in each midpoint of the sides, and one in the centroid), and the basis functions for the pressure are linear (one nodal point in the centroid and two derivatives), see Fig. 4.1a.

Next consider the finite-element approximation of w_i in Ω_2^0. The variational formulation of the elasticity equations contains only first-order partial derivatives so that linear basis functions based on the three vertices of the triangular element are sufficient to obtain a conforming finite-element approximation in Ω_2^0, see Fig. 4.1b. There are no additional constraints which force higher order polynomials to be used. Recall that the derivation of the variational form (3.7) imposed some conditions on the test functions at the interface G^0. In particular, we demanded that the restriction to G^0 of test functions in Ω_1^0 and Ω_2^0 should be identical, i.e., $\mathbf{v} = \mathbf{e}$ on G^0. When an extended quadratic polynomial function is used for the velocity approximation in Ω_1^0 and a linear basis function for the (scaled) displacements in Ω_2^0, a discretization as depicted in Fig. 4.2 is obtained. We

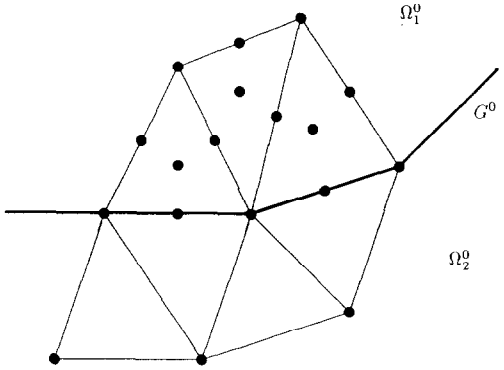

FIG. 4.2. Finite-element discretization.

note that special element types are required for elements which lie in Ω_2^0 and have one of their sides in common with the interfacial boundary G^0. This approach posed some problems, since the special elements could not be incorporated easily in the finite-element package we used (see Segal [20]). We therefore opted to use quadratic polynomial functions on triangular elements for the basis functions in Ω_2^0, thereby automatically satisfying the conditions imposed on the basis functions which lie on G^0.

The eigenvalue problem (4.8) is of the type often encountered when dealing with structural vibrations. In general, one is interested only in the eigenmodes corresponding to complex eigenvalues. Of those eigenmodes, the ones corresponding to the eigenfrequencies with the smallest imaginary parts are generally of principal engineering interest. Calculating the whole spectrum would then be a wasteful computational exercise. Schulkes and Cuvelier [21] found that if only a few eigenmodes are of interest, then these eigenmodes can be calculated efficiently using an inverse iteration procedure. This procedure will also be used in this paper; for details the reader is referred to the aforementioned paper.

5. NUMERICAL RESULTS

In order to obtain some insight into the types of normal modes inherent to the system, we consider the following

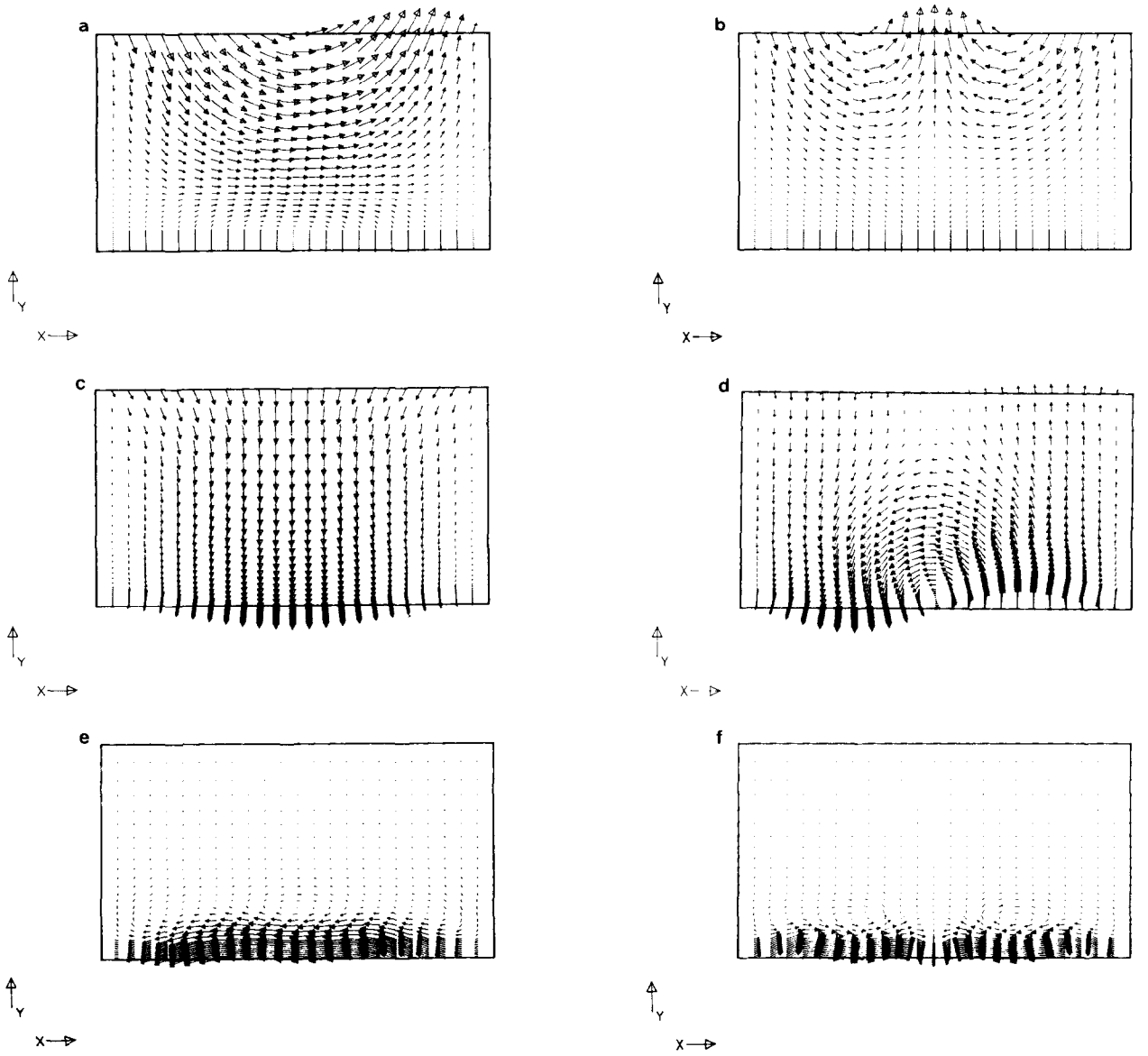

FIG. 5.1. Vector plots of the solution vector corresponding to the first and second free-surface modes (a, b), the first and second transverse structural-vibration modes (c, d), and the first and second longitudinal structural-vibration modes (e, f).

problem. A rectangular container of length $L = 1$, height $h = 1$, is half-filled with a viscous fluid with $Re = 50$. The side walls of the container are assumed rigid while the bottom of thickness $\delta = 0.05$ is assumed flexible with $\tilde{E} = 100$ and $\sigma = 0.25$. In Fig. 5.1a–f vector plots are shown of representative types of normal modes. The vector plots are made of the real parts of the components of the solution vector $(\mathbf{w}_f, \mathbf{w}_g, \mathbf{w}_e)^T$. The first and second free-surface oscillation modes are shown in Figs. 5.1a and b, respectively. Note that the free surface of the fluid is displaced significantly, but the flexible bottom is not effected noticeably by the fluid motion. Figures 5.1c and d show the first and second transverse oscillations modes of the structure. Observe that in the case of the first transverse mode the free surface of the fluid is also deflected significantly; the second transverse mode only slightly affects the free surface. In Fig. 5.1e and f vector plots are shown of the first and second longitudinal vibration modes. Observe that for the longitudinal modes a boundary layer forms in Ω_1 near the interfacial surface G^0.

As mentioned, the vector plots in Fig. 5.1 were obtained from the solution vector $(\mathbf{w}_f, \mathbf{w}_g, \mathbf{w}_e)^T$; that is, the plotted quantities in the solid refer to "velocity unknowns." We observe that the velocity vectors are continuous across the interfacial boundary G^0. Let us now re-scale the unknowns which refer to structured degrees of freedom such that they represent displacement rather than velocity vectors. Instead of just dividing the unknowns $\mathbf{w}_g$ and $\mathbf{w}_e$ by λ to obtain the vectors $\mathbf{d}_g$ and $\mathbf{d}_e$ which contain displacements, we re-scale as follows: $\mathbf{d}_g = (|\lambda|/\lambda)\,\mathbf{w}_g$ and likewise for $\mathbf{d}_e$. This is done in order to obtain the same order of magnitude for displacement and velocity vectors ($|\lambda|$ may be large). In all of the subsequent vector plots the structural unknowns are scaled is this way. Figures 5.2a and b show vector plots of the real and imaginary parts, respectively, of components of the re-scaled solution vector, corresponding to the second transverse structural vibration mode. In Fig. 5.2a we see that the elastic bottom is displaced downwards while the fluid velocity is upwards. Figure 5.2b shows a downward displacement of the elastic bottom; the fluid is directed downwards as well. The time-dependent motion of the system is a linear combination of the vector plots 5.2a and b.

The eigenfrequencies corresponding to the various types of oscillation modes will be investigated in some detail. Regarding the eigenvalues of the free-surface oscillations we found that they were hardly effected by the flexibility of the bottom; i.e., they are virtually identical if a similarly shaped rigid container is used. This is not surprising, since the vector plots show no interaction between the fluid and the solid, in which case the eigenfrequencies are given by expression (3.9). The eigenfrequencies of a freely-vibrating plate in a gravitational field are well known, cf. Landau and Lifshitz [15]. For a plate of thickness δ and length L we have, for the longitudinal waves,

$$\omega_n^{(l)} = \frac{n\pi}{L}\sqrt{\tilde{E}/(1-\sigma^2)}, \tag{5.1}$$

and, for the transverse waves, approximately

$$\omega_n^{(t)} = \sqrt{1 + \delta^2\tilde{E}/12(1-\sigma^2)[(2n+1)\pi/2L)]^4}. \tag{5.2}$$

In Fig. 5.3a we have plotted the imaginary parts of the eigenvalues corresponding to the transverse structural vibrations. The curve with squares corresponds to the

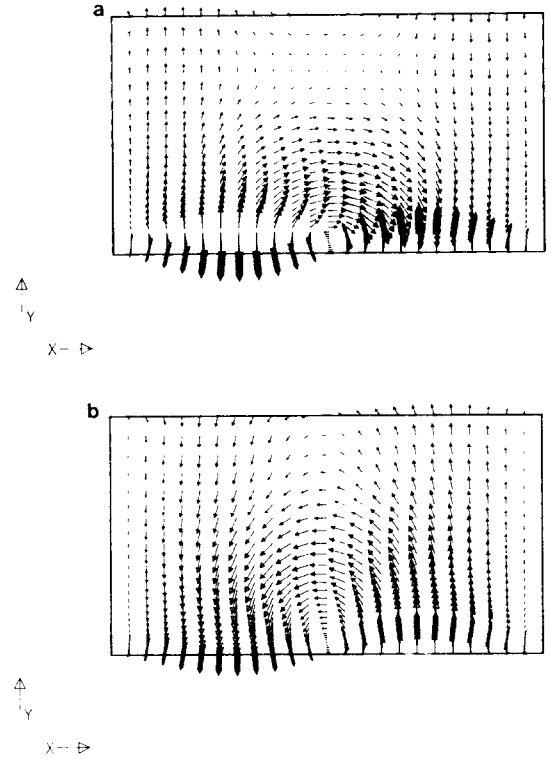

FIG. 5.2. Vector plots of the real (a) and imaginary (b) parts of fluid velocity and the (scaled) structural displacements corresponding to the second transverse structural vibration mode.

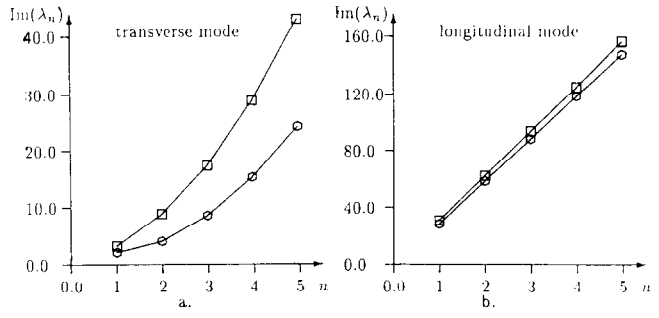

FIG. 5.3. Plots of Im(λ) for the transverse (a) and longitudinal (b) structural modes. The curves with squares correspond to the eigenvalues of a freely vibrating plate; the curves with circles are the numerical results of a plate in contact with a fluid.

analytical values of a freely vibrating plate given by (5.2); the curve with the circles corresponds to the numerical results of an oscillating plate in contact with a viscous fluid. We observe that the oscillation frequencies of a freely vibrating plate are higher than the corresponding modes of a plate in contact with a fluid. This is in agreement with the remarks made in Section 3, where we showed that the fluid inertia lowers the imaginary parts of the eigenvalues of structural vibration modes (Eq. (3.11)). Figure 5.3b shows a plot of the imaginary parts of the eigenvalues corresponding to the longitudinal oscillation modes. The curve with squares denotes, once again, the eigenvalues of a freely vibrating solid (5.1); the curve with the circles, those of a solid in contact with a fluid. We observe that the eigenvalues of a freely vibrating solid are again higher than those of the solid in contact with the fluid; however, the difference between the curves is less than in Fig. 5.3a. The reason is that the fluid is only slightly affected by longitudinal vibration modes, so that the fluid inertia term in (3.11) is small, resulting in Eq. (3.10).

Let us briefly reconsider the plots in Fig. 5.1e, f. Namely, the "wavy" shape of the solid in the case of the longitudinal vibration is of interest. Longitudinal vibrations of a freely vibrating plate do not display this transverse displacement super-imposed on the longitudinal motion so that the transverse displacement must be due to the presence of the fluid. Consider Fig. 5.1e in some more detail. We observe a slight transverse displacement with two maxima and two minima, i.e., a displacement akin to the fourth transverse vibration mode. One might expect that the presence of the fourth transverse vibration mode is due to the fact that the eigenfrequency of the first longitudinal mode is close to the eigenfrequency of the fourth transverse mode, resulting in a coupled modal vibration. This is indeed the case. However, with reference to Fig. 5.3 we note that the eigenfrequencies of a freely vibrating solid rather than those of the solid in contact with the fluid are the relevant frequencies to be considered. Namely, $\mathrm{Im}(\lambda) \approx 19$ for the fourth transverse mode of the solid in contact with fluid, while $\mathrm{Im}(\lambda) \approx 30$ for the freely vibrating solid and $\mathrm{Im}(\lambda) \approx 30$ for the first longitudinal mode. The mechanism behind the transverse motion is the pressure difference in the fluid which is the result of the fluid motion in the boundary layer near G^0. We point out that the phenomenon described above is due to the viscosity of the fluid. Neglecting viscous effects does not lead to fluid motion as a result of longitudinal vibrations, so that no pressure difference will be generated.

We next investigate the validity of the Tong-hypothesis. As was pointed out in Section 3, the Tong-hypothesis is exactly satisfied in one special case only; in all other cases it is an approximation. A number of authors, for example, Boujot [5] and Morand and Ohayon [8], have applied the Tong-hypothesis in their calculations. We are, however, not aware of an investigation (numerical or analytical) into the error introduced when the Tong-hypothesis is applied. It should be pointed out that, in case the Tong-hypothesis is not applied, the matrices **A**, **B**, and **C** in Eq. (4.8) have to be stored non-symmetrically, which may lead to storage difficulties when problems with a large number of degrees of freedom are considered. It is clearly advantageous when the Tong-hypothesis may be employed. In order to investigate the validity of the Tong approximation we consider an elastic hemispherical container fixed at the top. The radius of the outer boundary F is taken to be 1, the thickness of the container wall is $\delta = 0.1$ (see Fig. 5.4), and Poissons ration is $\sigma = 0.15$. A fluid with $Re = 200$ fills the container entirely. In Table II we present the eigenvalues of the first and second symmetric and anti-symmetric structural vibration modes for $\tilde{E} = 15$ and $\tilde{E} = 1500$. For both values of $\tilde{E}$ we have calculated the eigenvalues using the exact expression on G^0 (column 2) and using the Tong approximation (column 3). We observe first that invoking the Tong-hypothesis increases the eigenvalues and, in particular, the imaginary parts thereoff. Note also that the symmetric modes are affected less by the Tong-hypothesis than the anti-symmetric modes and that the effect of the Tong approximation diminishes for the higher modes. For $\tilde{E} = 1500$ we observe only a slight difference between the exact and approximate results. In

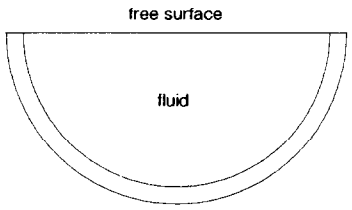

FIGURE 5.4

TABLE II

Eigenvalues for $\tilde{E}$

	$\tilde{E} = 15$	
	Without Tong	With Tong
1st anti-symm.	$-0.007 + 0.688i$	$-0.013 + 0.813i$
1st symm.	$-0.040 + 1.335i$	$-0.040 + 1.344i$
2nd anti-symm.	$-0.096 + 1.909i$	$-0.099 + 1.950i$
2nd symm.	$-0.150 + 2.677i$	$-0.150 + 2.701i$
	$\tilde{E} = 1500$	
	Without Tong	With Tong
1st anti-symm.	$-0.052 + 3.054i$	$-0.052 + 3.117i$
1st symm.	$-0.047 + 5.970i$	$-0.047 + 5.970i$
2nd anti-symm.	$-0.140 + 12.91i$	$-0.140 + 12.91i$
2nd symm.	$-0.180 + 21.76i$	$-0.180 + 21.77i$

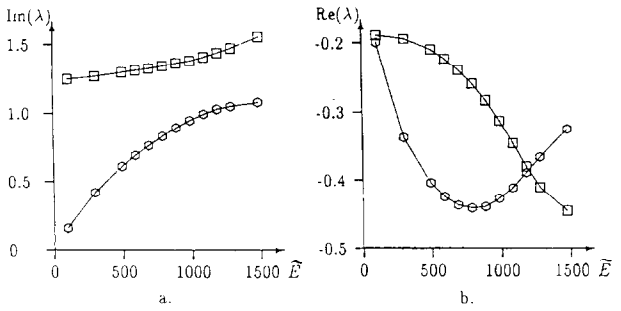

FIG. 5.5. Im(λ) and Re(λ) plotted against $\tilde{E}$ in (a) and (b), respectively.

fact, we found for $\tilde{E} \geqslant 1500$ that the boundary integral over G^0 could be neglected entirely without changing the eigenvalues by more than 3%. This might have been anticipated, since the energy required to displace the interface, characterized by the boundary integral over G^0, is small compared with the bending energy of the solid when $\tilde{E}$ is large. Thus, the question of whether or not the Tong-hypothesis may be applied is only important when $\tilde{E}$ is small.

In the last numerical experiment we consider a problem which is derived from the aerospace industry. In propellant tanks of spacecraft and satellites one has, in a number of cases, placed baffles on the sides of the tank. The aim of the baffles is to prevent the occurrence of excessive fluid sloshing during lift-off and flight and to keep the eigenfrequencies of the liquid (in particular, those of the lowest anti-symmetric modes) well separated from the eigenfrequencies of the spacecraft, see, for example, Abramson [22]. Numerous baffle types and shapes exist, ranging from rigid perforated rings to flexible slabs. Stephens [23] found that the damping coefficients of free-surface modes in tanks with flexible baffles mounted on the sides were larger than those in tanks without baffles or with rigid baffles.

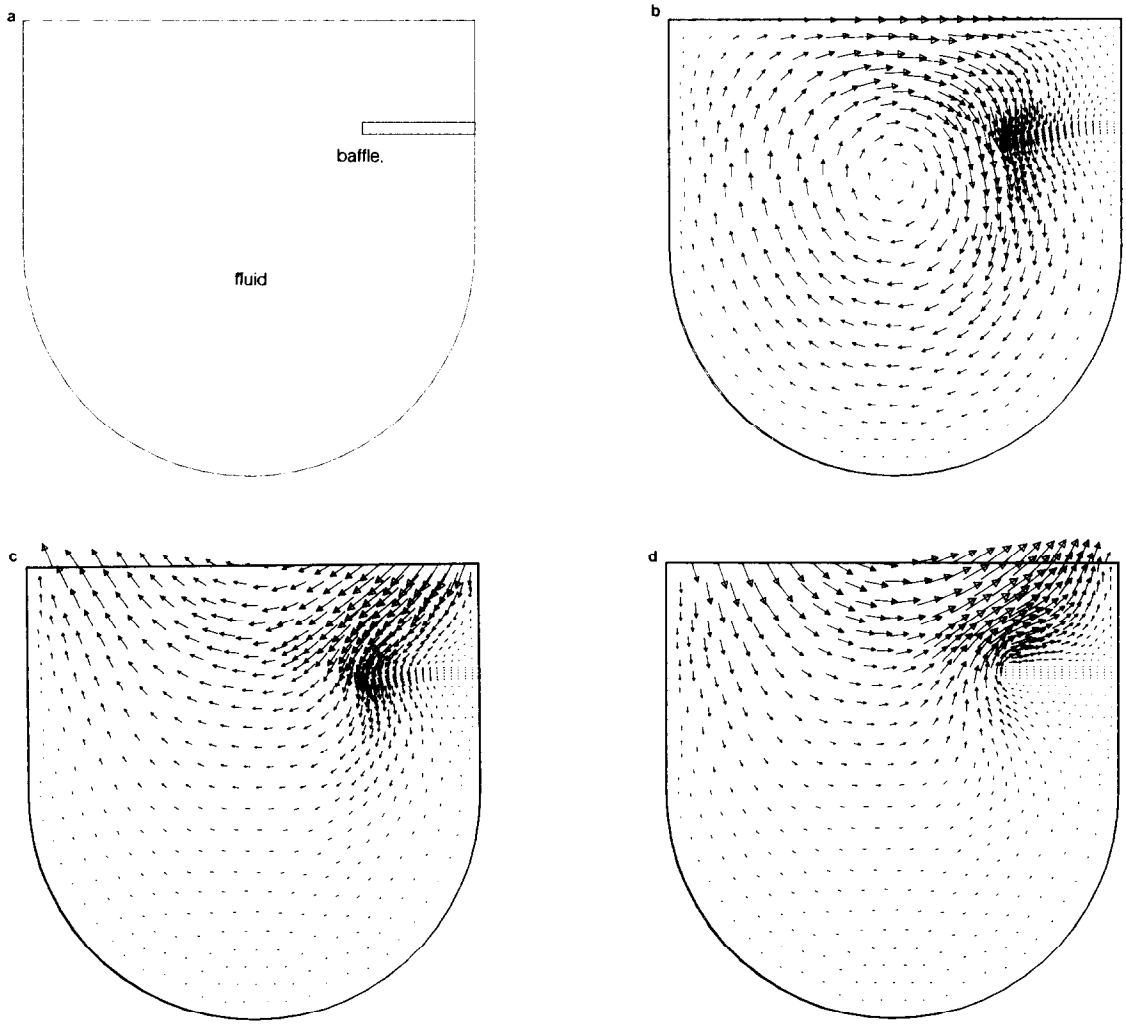

FIG. 5.6. Schematic diagram of a container with baffle (a). Vector plots of a baffle vibration mode for $\tilde{E} = 100$ (b), the first anti-symmetric surface mode for $\tilde{E} = 1000$ (c), and $\tilde{E} = 10^5$ (d).

Experimental tests showed that the damping coefficients were dependent on the rigidity of the baffle and, in fact, attained a maximum for a certain value of the rigidity.

To verify these results numerically, we consider a rectangular elastic baffle of length $L = 0.5$ and thickness $\delta = 0.05$, fixed to the side of a rigid container. The container consists of a rectangular top part and a hemispherical bottom of radius 1 (see Fig. 5.6a). For the fluid we take $Re = 50$ and Poisson's ratio is $\sigma = 0.25$. We consider the eigenvalues of the lowest eigenmodes of the system, i.e., the first free-surface mode and the lowest vibration mode of the baffle. In Fig. 5.5 the values of $\mathrm{Im}(\lambda)$ and $\mathrm{Re}(\lambda)$ have been plotted against $\tilde{E}$, for $\tilde{E}$ in the range $100 \leqslant \tilde{E} \leqslant 1500$. The values of $\mathrm{Im}(\lambda)$ on the curve with squares in Fig. 5.5a correspond to the values of $\mathrm{Re}(\lambda)$ on the curve with squares in Fig. 5.5b and likewise for the curves with circles. The dependence on $\tilde{E}$ of the curves of $\mathrm{Im}(\lambda)$ is typical of a system with two different oscillatory components, each of which depends on a common parameter. A branch corresponding to one type of modal vibrations changes over into a branch representing the other type of modal vibration as the common parameter, $\tilde{E}$ in this case, is varied (cf. Schulkes [12]). Here, for $\tilde{E} \leqslant 500$ the branch with the squares corresponds to the free surface modes, while for $\tilde{E} \geqslant 1300$ the branch with circles corresponds to free surface modes. For $\tilde{E} \approx 1000$ we have coupled free-surface and baffle vibrations. If one is interested in maximizing the damping coefficient of the first anti-symmetric fluid oscillation mode, it follows from Fig. 5.5b that the material properties of the baffle must be chosen such that $\tilde{E} \approx 1250$. Namely, for that value of $\tilde{E}$ the damping coefficient for the free-surface mode is -0.4; for all other values of $\tilde{E}$, the coefficient is larger and approaches -0.2 for values of $\tilde{E}$ far removed from the optimum value. Hence by an appropriate choice of the material properties of the baffle, the damping coefficient of the first anti-symmetric eigenmode can be increased by a factor of 2. In Fig. 5.6 vector plots are shown of a baffle vibration mode for $\tilde{E} = 100$ (b), and of the free-surface mode for $\tilde{E} = 1000$ (c) and $\tilde{E} = 10^5$ (d).

6. CONCLUSION

In this paper we have studied the interaction of a viscous fluid with an elastic solid. In particular, we have investigated the eigenmodes of the coupled fluid–structure system. Under the assumption that the so-called Tong-hypothesis holds, we have shown that oscillation modes exist with a number of different properties. First of all there exist fluid-oscillation modes. These modes are characterized by a small deflection of the structure and a large displacement of the fluid particles. Second, there exist normal modes is which the structure is deflected significantly, not affecting the fluid to a large extent. Finally, there are modes in which the fluid, as well as the structure, is displaced significantly. The existence of all three kinds of modes is verified numerically.

It was shown analytically that the extent to which the fluid affects the eigenvalues of the solid depends on the inertia of the fluid displaced by the solid. In all cases the fluid does lower the imaginary parts of the eigenvalues of the structural vibrations. Numerically we find that the presence of the fluid can lower the imaginary parts of the eigenvalues corresponding to the transverse vibration modes by up to 50%. Eigenvalues of the longitudinal modes are affected less by the presence of the fluid, due to the small fluid inertia term in that case.

The validity of the Tong-hypothesis is investigated numerically. It is found that application of the Tong-hypothesis increases the magnitude of the eigenvalues of the normal modes. The Tong-hypothesis mostly affects the lowest anti-symmetric eigenvalues. Symmetric modes and higher oscillation modes are affected less. Taking Young's modulus large enough also reduces the effect of the Tong-hypothesis.

We have shown numerically that there are cases in which the viscosity of the fluid plays an important role. This applies in particular longitudinal vibrations in the solid which create a boundary layer in the fluid adjacent to the fluid–solid interface. A pressure difference along the interfacial boundary, which is the result of the fluid motion, causes the solid to undergo a transverse displacement. In problems where damping coefficients of the system are to be found, it is obvious that viscous effects have to be included. Using one example, we have shown that with the approach presented in this paper one is capable of calculating the damping coefficients of a fluid–structure system.

ACKNOWLEDGMENTS

The author is grateful to Professor A. E. P. Veldman and Dr. C. Cuvelier for many enlighting discussions, and to the referees for helpful comments.

REFERENCES

1. W. K. Liu and H. G. Chang, *Comput. Struct.* **20** (1–3), 311 (1985).
2. T. Belytschko, *Nucl. Eng. Des.* **42**, 41 (1977).
3. J. W. Miles, *J. Appl. Mech.* **25**, 277 (1958).
4. C. W. Coale, *AIAA J.* **7** (2), 235 (1969).
5. J. Boujot, *J. Mec.* **11** (4), 649 (1972).
6. H. Berger, J. Boujot, and R. Ohayon, *J. Math. Anal. Appl.* **51**, 272 (1975).
7. M. A. Hamdi, Y. Ousset, and G. Verchery, *Int. J. Numer. Methods Eng.* **13**, 139 (1978).
8. H. Morand and R. Ohayon, *Int. J. Numer. Methods Eng.* **14**, 741 (1979).
9. T. C. Su, *J. Sound Vib.* **74** (2), 205 (1981).

10. A. C. Deneuvy, *Math. Modell. Numer. Anal.* **22** (1), 75 (1988).
11. P. Capodanno, *J. Mec.* **7** (1), 21 (1988).
12. R. M. S. M. Schulkes, *J. Eng. Math.* **24** (3), 237 (1990).
13. J. Sanchez Hubert and E. Sanchez Palencia, *Vibration and Coupling of Continuous Systems* (Springer-Verlag, Berlin, 1989).
14. P. Tong, ASQSR 66-0943, California Institute of Technology, 1966 (unpublished).
15. L. D. Landau and E. M. Lifshitz, *Theory of Elasticity* (Pergamon, Oxford, 1959).
16. N. D. Kopachevskii and A. D. Myshkis, *J. Phys. Math. Math. Phys.* **6** (6), 1054 (1966).
17. J. A. Deruntz and T. L. Geers, *Int. J. Numer. Methods Eng.* **12**, 531 (1978).
18. W. C. Müller, *Int. J. Numer. Methods Eng.* **17**, 113 (1981).
19. C. Cuvelier, A. Segal, and A. A. van Steenhoven, *Finite Element Methods and Navier–Stokes Equations* (Reidel, Dordrecht, 1986).
20. A. Segal, Programmers Guide, *SEPRAN Finite-Element Package* (Delft University of Technology, Delft, 1984).
21. R. M. S. M. Schulkes and C. Cuvelier, in *Lecture Notes in Physics*, Vol. 323, edited by M. Y. Hussaini (Springer-Verlag, Berlin, 1988), p. 528.
22. N. H. Abramson (Ed.), NASA SP-106 (1966).
23. D. G. Stephens, *AIAA J. Spacecr. Rockets* **5** (3), 765 (1966).